Electronic Supplemental Information

Characteristics and performance of rutile/anatase/brookite TiO_2 or TiO_2-$Ti_2O_3(H_2O)_2(C_2O_4)\cdot H_2O$ multiphase mixed crystal for catalytic degradation of emerging contaminants

Kangkai Hu,[a] Lei E,*[a, b] Dan Zhao,[a, b] Yajing Li, [c] Wei Zhao [a, b] and Hui Rong [a, b]

[a]School of Materials Science and Engineering, Tianjin Chengjian University, Tianjin, 300384, China.

[b]Tianjin Key Laboratory of Building Green Functional Materials, Tianjin Chengjian University, Tianjin, 300384, China.

[c]School of Environmental and Municipal Engineering, Tianjin Chengjian University, Tianjin, 300384, China.

*Corresponding author Tel: +86 150 2231 7560

E-mail: early@tcu.edu.cn

Experimental

1. Synthesis of the sample

A typical preparation process, a certain amount of potassium titanyl oxalate (PTO, A.R., 0.265 ~ 4.240 g) was dissolved in 30 mL deionized water to form a solution of 0.025 M at room temperature. Then, 3 mL hydrochloric acid (HCl, 37 wt%) was added into the solution, and the transparent precursor solution was formed after stirring uniformly. The precursor solution was transferred into an 80 mL Teflon-lined autoclave and heated at 150 °C for 12 h in an oven. After the hydrothermal reaction, the product was washed with deionized water to pH = 7 and dried at 65 °C. Through the above process, the TiO_2 or TiO_2-$Ti_2O_3(H_2O)_2(C_2O_4)\cdot H_2O$ mixed crystal was synthesized by in-situ growth. Table S1 showed the exact ratio of each component in the product.

Table S1 The exact ratio of each component in the product.

Sample	H_2O (mL)	Potassium titanyl oxalate (PTO)		HCl (mL)
		Mass (g)	Concentration (mol L^{-1})	
0.025 M	30	0.265	0.025	3
0.05 M	30	0.530	0.050	3
0.10 M	30	1.060	0.100	3
0.15 M	30	1.590	0.150	3
0.20 M	30	2.120	0.200	3
0.25 M	30	2.650	0.250	3
0.30 M	30	3.180	0.300	3
0.35 M	30	3.710	0.350	3
0.40 M	30	4.240	0.400	3

*The concentration in the table refers to the concentration of PTO solution formed by dissolving potassium titanyl oxalate in deionized water.

2. Characterization methods

a. Field emission scanning electron microscopy (FESEM)

The micro morphology of the sample was observed by field emission scanning electron microscope (FESEM, JSM-7800F, Japan), and a large area energy dispersive spectrometer (EDS, X-Max^N, Britain) was used to analyze the composition of the sample, the acceleration voltage was 10 kV, and the test environment was high vacuum.

b. X-ray diffraction (XRD)

The phase structure of the sample was characterized with X-ray diffraction (XRD, D/MAX-Ultima IV, Japan), with a source of Cu-K_α radiation ($\lambda = 1.54056$ Å). The voltage and current of the tube were 40 kV and 40 mA, respectively. The step length was 0.02° with scan rate of 10° min^{-1} from 10° to 80°. The crystallite size was calculated according to the Scherrer equation, that is equation (1).[1]

$$D = K\lambda/(\beta\cos\theta) \qquad (1)$$

Where λ is the wavelength of X-ray radiation (Cu-K_α = 0.15405 nm); K is advisable 0.89; β is the full width at the half-maximum and θ is the diffraction angle.

c. Fourier transform infrared spectroscopy (FTIR)

Fourier transform infrared spectroscopy (FTIR, Thermo Nicole 380, America) was used to determine the changes of surface functional groups of the sample with the wavenumber range of 4000~400 cm^{-1}, and KBr (G.R.) as a reference.

d. Ultraviolet-Visible absorption (UV-vis)

The UV-vis absorption spectra was studied by UV-vis spectrometry (PerkinElmer Lambda 750 UV/Vis/NIR Spectrometer, America) equipped with an integrating sphere attachment using $BaSO_4$ (G.R.) as background from 300 nm to 500 nm in room temperature.

e. Mott-Schottky, current-potential curves (I-V) and electrochemical impedance spectroscopy (EIS)

The PEC test was performed in a three-electrode system by the CHI 760E electrochemical workstation, and a 0.5 M Na_2SO_4 solution (pH = 7) was selected as the electrolyte solution. The sample to be tested was used as a working electrode, the platinum electrode was used as a counter electrode, and the Ag/AgCl electrode was used as a reference electrode. The solar simulator light source was a long arc xenon lamp with AM 1.5G (100 mW cm^{-2}) standard filter produced by Beijing Heng Gong Instrument Co., Ltd. The measured potential (vs. Ag/AgCl) was converted to the reversible hydrogen electrode (RHE) scale using the Nernst equation (2).[2, 3]

$$E_{RHE} = E_{Ag/AgCl} + 0.0591 * pH + E_{Ag/AgCl}' (3.0\ M\ KCl) \qquad (2)$$

Where $E_{Ag/AgCl}'$ (3.0 M KCl) is 0.1976 V at 25 ℃. The calculation of the capacitance C in the Mott-Schottky curve uses the formula (3).[4, 5]

$$C = -1 / (2\pi f Z'') \qquad (3)$$

Where f is the frequency during the test.

f. Brunauer-Emmett-Teller nitrogen adsorption (BET)

The specific surface area and pore size distribution of the samples was characterized with Brunauer-

Emmett-Teller nitrogen adsorption method (BET, Nova 3000e, America), and the test temperature was 77.3 K.

g. X-ray photoelectron spectroscopy (XPS)

The surface elements and their chemical states were characterized by X-ray photoelectron spectroscopy (XPS, Thermo ESCALAB 250Xi, America) with the energy analysis range of 0~1200 eV.

h. Photocatalytic experiment

The photocatalysis degradation of methyl orange (MO) and hydroxybenzoic acid (HBA) was used to investigate the photocatalytic activity of the samples. The reaction temperature was maintained at room temperature. Typically, 0.05 g photocatalyst powders were placed in 25 mL MO (20 mg L^{-1}, pH = 3) or HBA (20 mg L^{-1}, unadjusted pH) and the suspension was stirred in the dark for a certain time to ensure adsorption/desorption equilibrium before light on. After the sample was put into the multi-channel photocatalytic reaction system (PCX-50C Discover, China) under UV-light irradiation (5 W, λ_{max} = 365 nm), the absorbance of MO or HBA was measured at a given time intervals, with UV-vis absorption spectra at maximum absorption wavelengths (λ_{MO} = 505 nm, λ_{HBA} = 298 nm). Finally, the photocatalytic activity of the product was characterized through photocatalysis degradation (η) determined by using the following equation (4).

$$\eta = (1 - A_t/A_0) \times 100\% = (1 - C_t/C_0) \times 100\% \quad (4)$$

Where A_0 and A_t are the initial and final MO concentrations, respectively. The kinetic rate of photocatalytic reaction for low concentrations of MO were estimated from the pseudo first-order linear fitting relationship diagram of $\ln(C_0/C_t)$ against illumination time.[6]

i. Surface photovoltage spectroscopy (SPV)

The optical absorption properties of the samples were conducted by the surface photovoltage spectroscopy (SPV, PL-SPS/IPCE 1000, China) in air ambient at room temperature with the wavelength range of 300-600 nm.

j. Heat treatment of the sample

The heat treatment temperature-time curve of the sample is shown in Fig. S1, where Rt is room temperature and C_{end} represents the final temperature. The time relationship is as follows:

$$t_2 = t_1 + 60 \quad (5)$$

$$t_4 = t_3 + 120 \quad (6)$$

Fig. S1 The heat treatment temperature-time curve of the sample.

Fig. S2 SEM images of the 0.15 M sample at 180 °C for 12 h. (a) Sample plots at low magnification, (b) high magnification diagram of the tagged area in (a).

Fig. S3 XRD spectra of 0.20 M sample after heat-treated at 400 ℃ for 2 h.

Fig. S4 Crystallite size of the sample prepared with different PTO concentration.

Fig. S5 Mott-Schottky plots of the sample.

Fig. S6 Average particle size distribution of 0.15 M sample after heat-treated at different temperature.

Fig. S7 Recycling photodegradation MO of un-heated 0.15 M under UV-light irradiation.

Fig. S8 Degradation pathway of HBA by photocatalyst under UV-light irradiation.

Fig. S9 PEC curves of the sample. SPV spectrum (a), the phase angle (b), I-V curves (c) and EIS spectra (d).

Fig. S10 The energy band structure of rutile and anatase TiO_2.[7, 8]

Video 1 The stick model of $Ti_2O_3(H_2O)_2(C_2O_4)\cdot H_2O$.

Video 2 The polyhedral model of $Ti_2O_3(H_2O)_2(C_2O_4)\cdot H_2O$.

Video 3 The polyhedral model of rutile TiO_2.

Video 4 The polyhedral model of anatase TiO_2.

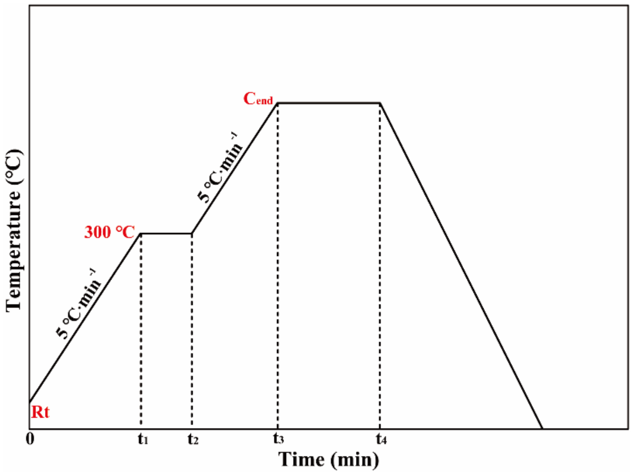

Fig. S1 The heat treatment temperature-time curve of the sample.

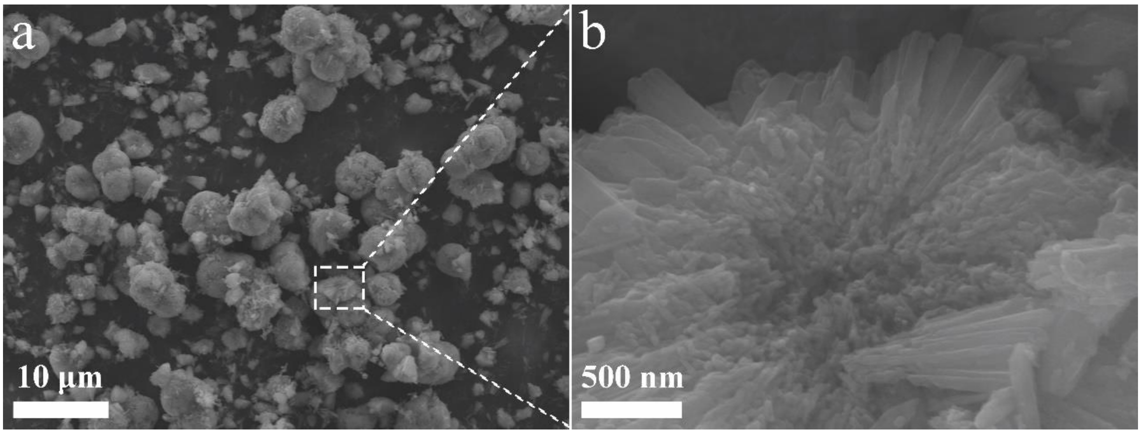

Fig. S2 SEM images of the 0.15 M sample at 180 °C for 12 h. (a) Sample plots at low magnification, (b) high magnification diagram of the tagged area in (a).

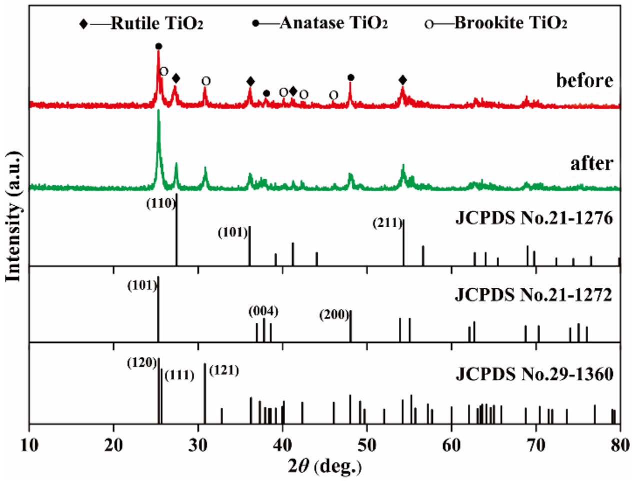

Fig. S3 XRD spectra of 0.20 M sample after heat-treated at 400 °C for 2 h.

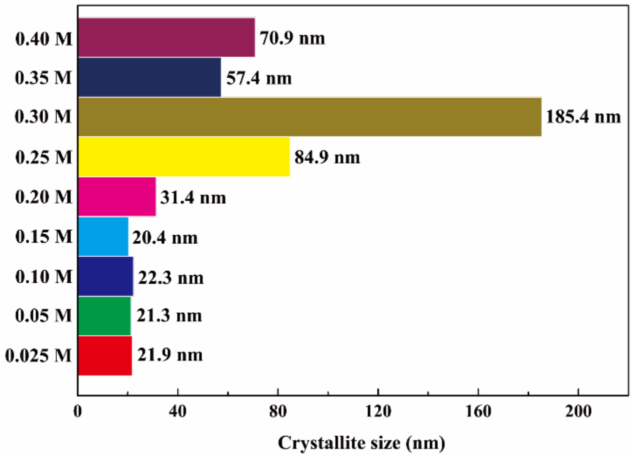

Fig. S4 Crystallite size of the sample prepared with different PTO concentration.

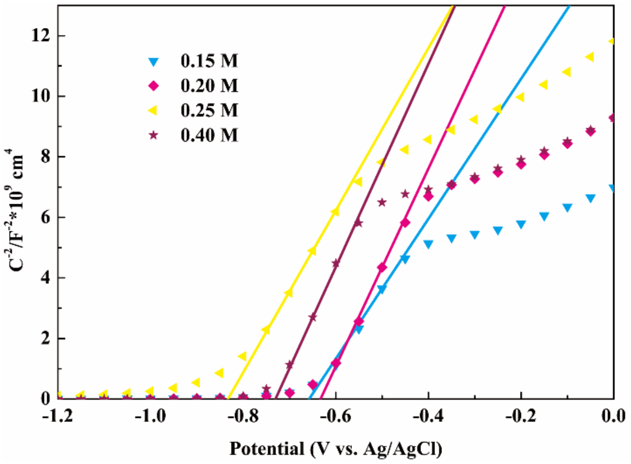

Fig. S5 Mott-Schottky plots of the sample.

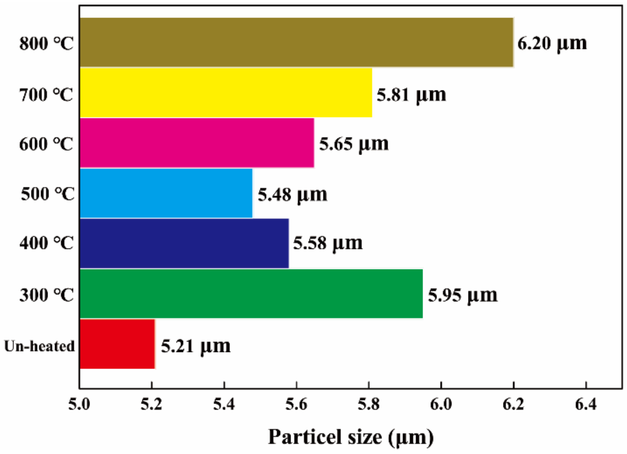

Fig. S6 Average particle size distribution of 0.15 M sample after heat-treated at different temperature.

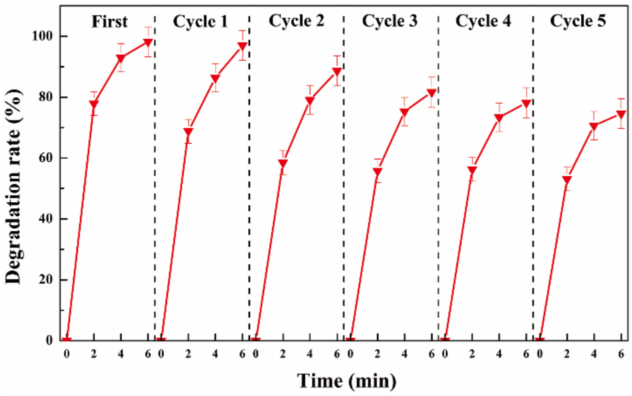

Fig. S7 Recycling photodegradation MO of un-heated 0.15 M under UV-light irradiation.

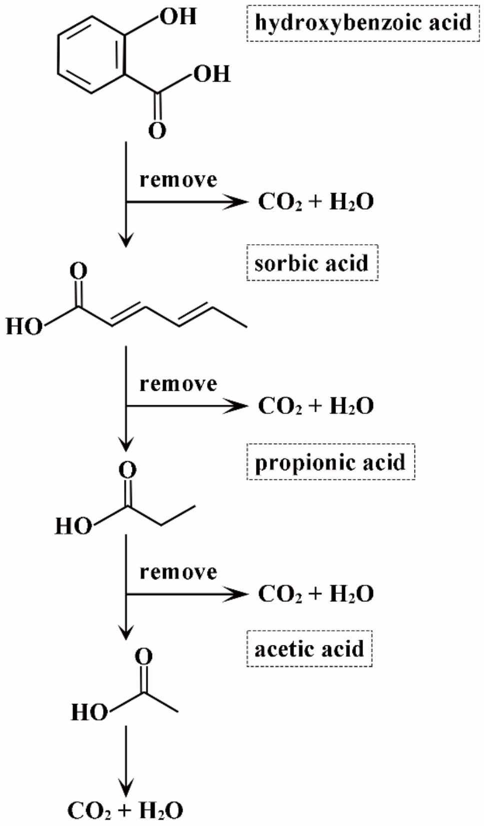

Fig. S8 Degradation pathway of HBA by photocatalyst under UV-light irradiation.

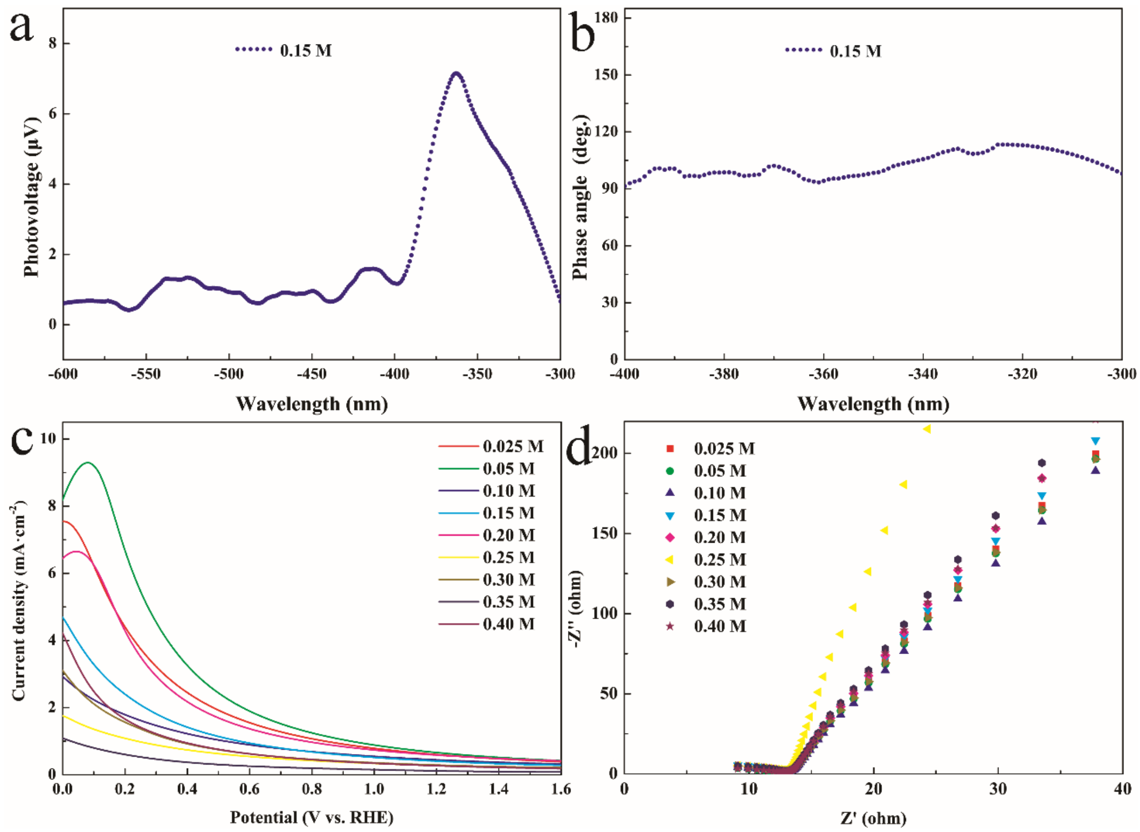

Fig. S9 PEC curves of the sample. SPV spectrum (a), the phase angle (b), I-V curves (c) and EIS spectra (d).

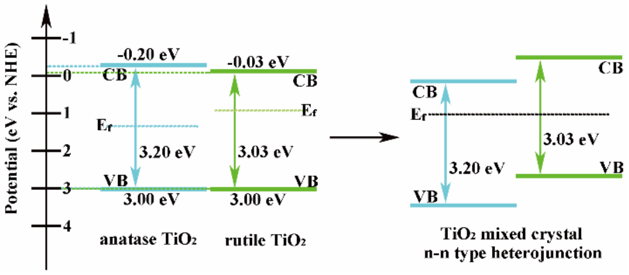

Fig. S10 The energy band structure of rutile and anatase TiO_2.[7, 8]

References

1. K. Hu, L. E, D. Zhao, C. Hu, J. Cui, L. Lai, Q. Xiong and Z. Liu, *CrystEngComm*, 2018, **20**, 3363-3369.
2. Y. Li, L. Zhang, A. Torres-Pardo, J.M. González-Calbet, Y. Ma, P. Oleynikov, O. Terasaki, S. Asahina, M. Shima, D. Cha, L. Zhao, K. Takanabe, J. Kubota and K. Domen, *Nat. Commun.*, 2013, **4**, 2566.
3. J. Wei, C. Zhou, Y. Xin, X. Li, L. Zhao and Z. Liu, *New J. Chem.*, 2018, **42**, 19415-19422.
4. R.M. Fernández-Domene, E. Blasco-Tamarit, D.M. García-García and J. García Antón, *J. Electrochem. Soc.*, 2013, **161**, C25-C35.
5. F. Fabregat-Santiago, G. Garcia-Belmonte, J. Bisquert, P. Bogdanoff and A. Zaban, *J. Electrochem. Soc.*, 2003, **150**, E293-E298.
6. P. Dong, Y. Wang, B. Cao, S. Xin, L. Guo, J. Zhang and F. Li, *Appl. Catal. B-Environ.*, 2013, **132-133**, 45-53.
7. Y. Hu, D. Z. Li, Y. Zheng, W. Chen, Y. H. He, Y. Shao, X. Z. Fu and G. C. Xiao, *Appl. Catal. B-Environ.*, 2011, **104**, 30-36.
8. D.O. Scanlon, C.W. Dunnill, J. Buckeridge, S.A. Shevlin, A.J. Logsdail, S.M. Woodley, C.R. Catlow, M.J. Powell, R.G. Palgrave, I.P. Parkin, G.W. Watson, T.W. Keal, P. Sherwood, A. Walsh and A.A. Sokol, *Nat. Mater.*, 2013, **12**, 798-801.